Polymer 50 (2009) 2762–2767

Contents lists available at ScienceDirect

Polymer

journal homepage: www.elsevier.com/locate/polymer

Xanthene dyes/amine as photoinitiators of radical polymerization: A comparative and photochemical study in aqueous medium

M.V. Encinas [a,*], A.M. Rufs [a], S.G. Bertolotti [b], C.M. Previtali [b]

[a] Facultad de Química y Biología, Universidad de Santiago de Chile, Casilla 307-2, Santiago, Chile
[b] Departamento de Química, Univ. Nacional de Río Cuarto, Argentina

ARTICLE INFO

Article history:
Received 8 March 2009
Received in revised form
6 April 2009
Accepted 11 April 2009
Available online 23 April 2009

Keywords:
Xanthene dye photoinitiators
Aqueous photopolymerization
Relation between photochemistry and photoinitiation

ABSTRACT

The efficiency of several xanthene dyes as photoinitiators of the free radical polymerization in aqueous medium was evaluated. These results show that dyes with triplet quantum yield higher than 0.1 present similar efficiencies, independently of their different chemical structure. A detailed study of the photophysics of the dyes under the polymerization conditions was carried out using laser time-resolved spectroscopies. These studies show that the active radicals are those which formed in the interaction of excited triplet state of the dye with the amine through an electron transfer process. In spite of this, the photoinitiation efficiency is not correlated with the triplet quantum yield. Also, the photophysics studies show that the quantum yield of the different pathways of the decomposition of the charge transfer intermediate is an important parameter to predict the efficiency of these photoinitiator systems. The experimentally measured active radical formation is well correlated with that calculated from the polymerization rate. The presence of heavy atoms in the xanthene ring increases the triplet quantum yield, but decreases the active radical yield, and then the polymerization rate.

1. Introduction

The extension of the absorption spectrum of photoinitiators to the visible light is now of great interest. Besides of the practical interest of using light in this spectral region, they are found applications that range from lithography for integrated circuit manufacture to curing processes. Dye-sensitized photopolymerization of vinyl monomers has been the subject of extensive investigations. Many of these systems consist of a dye and amines as reducing agents, where the excited triplet state of the dye acts as the oxidizing species [1–4]. Several dyes are been used as photoinitiators, however, there are no systematic studies that allow to predict their relative efficiencies.

Xanthene dyes are very convenient visible photoinitiators due to their high absorption in the region 500–580 nm, and their wide solubility range. Furthermore, this absorption range makes these dyes as suitable photoinitiators for pulsed-laser polymerization using the second harmonic of the Nd:YAG laser, 532 nm. Eosin and Rose Bengal in the presence of electron donors such as tertiary amines, *N*-phenylglycines, and sulfur containing compounds have been described as efficient photoinitiators for the free radical polymerization of acrylate monomers [5–13]. Also, Fouassier et al. have shown that xanthene dyes are efficient photosensitizers in multicomponent photoinitiator systems [14,15]. Xanthene derivatives, in particular fluorone dyes, in conjunction with amines or borates as reducing agents have been developed for use as visible photoinitiators for polymerization of acrylic monomers [16–19]. More recently, eosin in the presence of amine has been used as efficient photoinitiator for surface modification by surface-mediated polymerization [20]. In all these systems it has been proposed that the active free radicals are formed in one-electron transfer process from the electron donor co-initiator to the excited triplet of the dye. Because the active radical formation involves a charge transfer intermediate, the photoinitiation efficiency is markedly sensitive to the nature of the dye. The photochemical properties of various xanthene dyes have been the subject of several studies [6,9,10,14,16]. However, a correlation between the photochemistry and the initiation efficiency requires the detailed photochemical study under the polymerization conditions.

In this work we compare the efficiency of several xanthene dyes, shown in Scheme 1, as photoinitiators of the polymerization of acrylamide in aqueous solution. Triethanolamine (TEOHA) was

* Corresponding author. Tel.: +56 2 7181141; fax: +56 2 6812108.
E-mail address: maria.encinas@usach.cl (M.V. Encinas).

0032-3861/$ – see front matter © 2009 Elsevier Ltd. All rights reserved.
doi:10.1016/j.polymer.2009.04.024

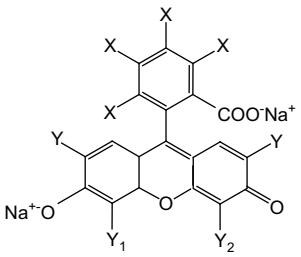

X	Y	Y_1	Y_2	Dye
H	Br	Br	Br	eosin Y
Cl	I	I	I	Rose Bengal
H	I	I	I	erythrosin B
H	Br	HgOH	H	mercury dibromofluorescein
H	H	Br	Br	4,5-dibromofluorescein
H	H	H	H	fluorescein

Scheme 1. Structure of xanthene dyes.

used as co-initiator. The photophysics and photochemistry of the dyes under the polymerization conditions were investigated, and correlated to their efficiency as photoinitiators.

2. Experimental part

2.1. Material

Triethanolamine (TEOHA) (Aldrich) was purified by distillation under reduced pressure prior to use. All dyes were obtained from Aldrich and were used as received. Acrylamide from Sigma (electrophoretic grade >99%) was used as received.

2.2. Measurements

Acrylamide polymerization rates (Rp) were measured dilatometrically in oxygen-free aqueous solutions at 25 °C. The pH was adjusted at 9.5 by NaOH or HCl addition. The monomer concentration was 0.4 M. The samples were irradiated at 532 nm using as light source a xenon lamp–monochromator system. Low absorbances (0.1) of dyes were used to avoid the aggregation of the dyes. The polymerizations were carried out to conversion below 25%.

Absorption spectra were measured using an HP8453 diode array spectrophotometer. Static fluorescence measurements were obtained on a Spex Fluorolog spectrofluorometer in air equilibrated solutions at 20 °C. Bandwidths of 1.25 nm were used for excitation and emission slits. Fluorescence lifetimes were measured with an Edinburgh Instrument OB-900 time correlated single photon counting fluorometer (Edinburgh, UK). Analysis of the fluorescence decays was carried out by a least-square iterative de-convolution method using the analysis routine provided by Edinburgh Instrument.

Transient absorption measurements were made using a laser flash photolysis (LFP) equipment. The third harmonic of an Nd:YAG laser (532 nm, 10 mJ/pulse, 20 ns) was employed for sample excitation. The signals from the monochromator/photomultiplier system were initially captured by a HP54504 digitizing oscilloscope and transferred to a computer for storage and analysis. For experiments in the presence of TEOHA a flow cell was used to avoid sample photolysis by the laser flash.

Laser-induced-opto-acoustic-spectroscopy (LIOAS) measurements were done with the same laser used for LFP with the beam width shaped to a rectangular slit (0.5 mm w × 5 mm h). The details of our LIOAS set-up have been reported elsewhere [21,22]. A time resolution of the LIOAS experiments from *ca.* 20 ns up to 3 μs using de-convolution techniques could be achieved.

3. Results and discussion

3.1. Polymerization studies

The polymerization of acrylamide photoinitiated by several xanthene dyes in aqueous solution at pH 9.5 was carried out with visible light of 532 nm at 25 °C. In order to compare the photoinitiation efficiency of the different kinds of dyes we also measured, under the same experimental conditions, the acrylamide polymerization rate photoinitiated by resorufin, a phenoxazine dye, the phenazinium dyes, safranin and phenosafranin, and rhodamine 6G, an amine xanthene dye. These dyes present a high absorption at 532 nm and their behaviour as photoinitiators has been previously studied by us [23–25]. The measurements were made in solutions with matched absorbances of near 0.1 at 532 nm with 10 mm pathlength. Under this condition no evidence was found for aggregate formation in any of the dyes. The acid–base equilibrium of xanthene dyes in ground and excited states has been reported [26–29]. According to these reports, at the polymerization conditions, pH 9.5, all xanthene dyes exist in the dianionic form in the ground state as well as in the excited states. Possible pH effects on the polymerization of acrylamide in aqueous solution were examined using 4,4′-azobis (2-amidinopropane) dihydrochloride (ABAP) as photoinitiator. These results showed that the polymerization rate measured at several pHs was kept constant in the pH range 3–10. At high acid or high basic media the polymerization rate decreases considerably, as expected from the hydrolysis of the amide group.

Absorption spectra of studied xanthene dyes in water at pH 9.5 are shown in Fig. 1.

The polymerization was negligible when the dyes and monomer were irradiated in the absence of amine. However, it was efficiently activated by the presence of TEOHA. It is well known that xanthene dyes present photobleaching when are irradiated in the presence of amines [30,31]. We found that the concentration of xanthene dyes in the presence of TEOHA before and after the steady state irradiation, at the same experimental conditions

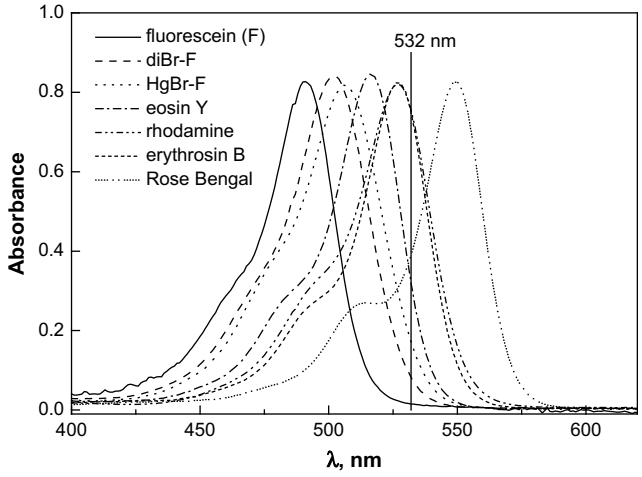

Fig. 1. Absorption spectra of xanthene dyes in water pH 9.5.

where the polymerizations were carried out, decreases ~20%. However, when these experiments were carried out in the presence of acrylamide showed that the photobleaching is inhibited by the monomer.

The polymerization rates, obtained from the initial slope of plots of the volume contraction vs. time, increase with the amine concentration and reach a maximum value at ~15 mM amine. Further amine addition slightly inhibits the polymerization. This behaviour holds for all studied xanthene dyes. Typical plots of Rp vs. TEOHA concentration are shown in Fig. 2, and Rp values at 20 mM TEOHA are colleted in Table 1. These data show that fluorescein and rhodamine 6G do not lead to polymer, and Rp for the other studied xanthene dyes present very small differences.

Data of Table 1 also show that the xanthene dyes that lead to polymer formation behave as more efficient photoinitiators when compared to phenoxazine and phenazine dyes. Also, it is interesting to note that a similar trend in the photoinitiation efficiency has been reported for the polymerization of diacrylates employing eosin, Rose Bengal and phenosafranin as photoinitiators [14].

As described for the free radical polymerization of vinyl monomers in aqueous medium photoinitiated by bimolecular systems with amines as co-initiator, Rp can be expressed by the classical kinetic law [24,32,33], given by

$$\mathrm{Rp} = \left(\frac{k_\mathrm{P}}{k_\mathrm{t}^{1/2}}\right)\Phi_\mathrm{i}^{1/2} I_\mathrm{a}^{1/2}[\mathrm{M}] \tag{1}$$

where I_a is the intensity of the absorbed light by the photoinitiator, and Φ_i is the initiation quantum yield. From Eq. (1) it can be deduced that at the same monomer concentration, the same solvent, and identical I_a, the dependence of Rp with the chemical structure of the photoinitiator will be consequence only of the initiation quantum yield. Thus, Eq. (1) indicates that under the same experimental conditions, the relative photoinitiation efficiency will be given by the ratio of the square of polymerization rates, Eq. (2)

$$\frac{(\Phi_\mathrm{i})_1}{(\Phi_\mathrm{i})_2} = \frac{(\mathrm{Rp})_1^2}{(\mathrm{Rp})_2^2} \tag{2}$$

Therefore, in order to understand the efficiencies of the different dyes, knowledge of the factors that control the initiation quantum yield is necessary. To this goal an investigation of the photophysical and photochemical behaviour of the dyes under polymerization conditions is mandatory.

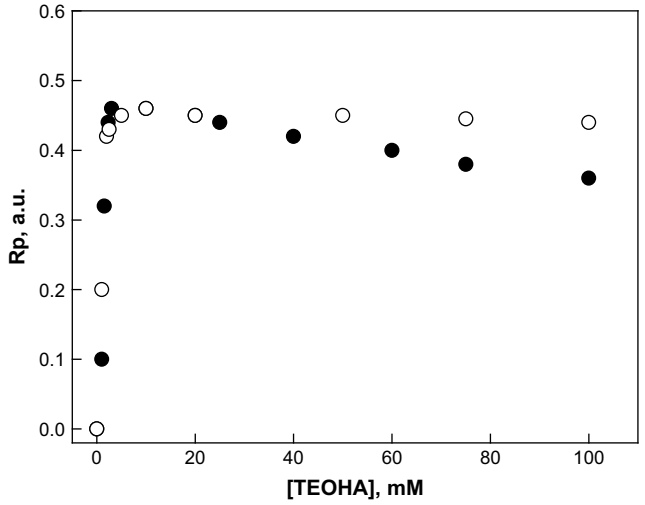

Fig. 2. Polymerization rates photoinitiated by (○) erythrosine B, and (●) mercury dibromofluorescein, as function of the TEOHA concentration. Acrylamide = 0.4 M, in water pH 9.5 at 25 °C. Excitation at 532 nm.

Table 1
Polymerization rates of acrylamide photoinitiated by dyes irradiated at 532 nm in the presence of 20 mM TEOHA, water at pH 9.5.

Dye	Rp (arbitrary units)
Mercury dibromofluorescein	0.45
Eosin Y	0.41
Rose Bengal	0.44
Erythrosin B	0.45
4,5-Dibromofluorescein	0.46
Fluorescein	NP
Rhodamine 6G	NP
Phenosafranin	0.33
Safranin O	0.22
Resorufin	0.15

NP = no polymer formed.

3.2. Photochemical studies of the initiation mechanism

It is well known that the deactivation of excited states of xanthene dyes by amines involves the formation of a charge transfer intermediate between the excited dye and the amine with the latter acting as an electron donor [6,9,10,12,14,34–36]. The deactivation processes can be represented through Eqs. (3)–(8)

$$\mathrm{Dye}^{2-} + \mathrm{h}\nu \rightarrow {}^1(\mathrm{Dye}^{2-})^* \tag{3}$$

$${}^1(\mathrm{Dye}^{2-})^* \rightarrow \text{deactivation} \tag{4}$$

$${}^1(\mathrm{Dye}^{2-})^* + \mathrm{Am} \rightarrow \text{quenching} \tag{5}$$

$${}^1(\mathrm{Dye}^{2-})^* \rightarrow {}^3(\mathrm{Dye}^{2-})^* \tag{6}$$

$${}^3(\mathrm{Dye}^{2-})^* + \mathrm{Am} \rightarrow [(\mathrm{Dye}^{2-})^{\bullet -}\mathrm{Am}^{\bullet +}] \tag{7}$$

$${}^3(\mathrm{Dye}^{2-})^* \rightarrow \text{deactivation} \tag{8}$$

The main decomposition steps of the charge transfer intermediate are the back electron transfer to give the dye and the amine in the ground state (Eq. (9)), and the proton transfer from the amine cation radical to the dye anion radical giving the monoprotonated dye radical ($(\mathrm{DyeH}^{2-})^\bullet$) and the neutral α-aminoalkyl radical ($\mathrm{Am}(-\mathrm{H})^\bullet$), (Eq. (10)). The amine neutral radical is the active radical for the polymerization initiation.

$$[(\mathrm{Dye}^{2-})^{\bullet -} + \mathrm{AmH}^{\bullet +}] \rightarrow \mathrm{Dye} + \mathrm{Am} \tag{9}$$

$$[(\mathrm{Dye}^{2-})^{\bullet -} + \mathrm{AmH}^{\bullet +}] \rightarrow (\mathrm{DyeH}^{2-})^\bullet + (\mathrm{Am}(-\mathrm{H})^\bullet \tag{10}$$

Frequently, it is proposed that active radicals are formed from the interaction of the excited triplet state with the amine; the singlet interaction inhibits the polymerization. From the above mechanism the amine radical quantum yield ($\Phi_{\mathrm{Am}^\bullet}$) is given by Eq. (11)

$$\Phi_{\mathrm{Am}^\bullet} = \Phi_\mathrm{T} f_\mathrm{T} \alpha \tag{11}$$

where f_T is the fraction of triplets quenched by the amine, α is the fraction of quenched triplets that lead to radicals (reaction (10)), and Φ_T stands for the intersystem crossing quantum yield in the presence of amine given by

$$\Phi_T = \frac{\Phi_T^o}{({}^S k_q \tau_S^o [Am] + 1)} \quad (12)$$

where Φ_T^o is the intersystem crossing quantum yield in the absence of amine, ${}^S k_q$ is the singlet quenching rate constant, and τ_S^o is the singlet lifetime in the absence of amine.

The parameter f_T is related to the triplet quenching rate constant (${}^3k_q$) by Eq. (13), where k_o is the triplet decay rate constant in the absence of the amine.

$$f_T = \frac{{}^3k_q[Am]}{{}^3k_q[Am] + k_o} \quad (13)$$

These relations show that to predict the radical quantum yield, and hence the polymerization efficiency, it is required to know the singlet and triplet lifetimes as well as quantum yields and the rate constants of the different pathways that deactivate the excited states.

3.3. Photophysical parameters and photochemical processes

3.3.1. Singlet state

Singlet state lifetimes were determined by the singlet photon counting technique in air equilibrated solutions at pH 9.5, and are collected in Table 2.

The comparison of singlet lifetime values with those previously reported is difficult because they are very dependent on the solvent and the pH. Data of Table 2 show that the singlet lifetime under the polymerization conditions, aqueous solution at pH 9.5, are rather shorter than those reported in organic media [26,37–39]. In the presence of TEOHA the emission is quenched without spectral distortion. Rate constants for singlet quenching were obtained from the shortening of the fluorescence lifetime by gradual amine addition and are also shown in Table 2. The values are near the diffusion control limit. Values for Rose Bengal and erythrosin could not be determined due to the very short lifetime (ca. 100 ps), as expected from the fast intersystem crossing process. In these cases assuming a diffusion controlled rate constant value ($4\times10^9\ M^{-1}\ s^{-1}$) for the singlet quenching, the fraction of the excited singlet states intercepted by TEOHA 20 mM is less than 1%.

3.3.2. Triplet state

Laser flash photolysis experiments of xanthene dyes in water at pH 9.5 gave a transient absorption spectrum that presents two bands in the regions of 340–470 and 550–700 nm, that are assigned to the triplet state. At pH 9.5 it can be considered that the dominant form of the triplet state of the dyes is the dianionic form [26]. Fig. 3 shows the absorption spectrum of 4,5-dibromofluorescein in Ar-saturated aqueous solution pH 9.5 at 5 μs after the laser pulse. The depression of the absorption corresponds to the bleaching of the ground state absorption of the dye. Similar spectra were obtained for all dyes. The spectra of eosin and Rose Bengal show similar characteristics to those previously reported in aqueous solution at neutral pH or in water–organic solvent mixture [40,41].

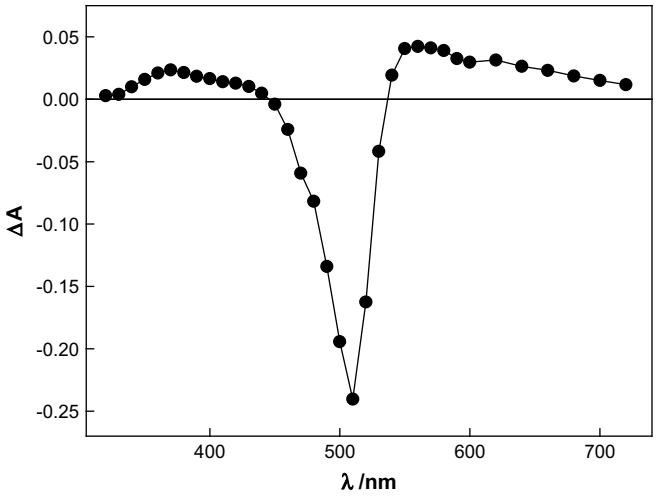

Fig. 3. Transient absorption spectrum of 4,5-dibromofluorescein in water at pH 9.5, taken at 5 μs after the laser pulse.

In order to obtain the triplet quantum yields Φ_T, two independent techniques were employed. The first is based on measurements by the LFP technique of the product of the triplet quantum yield and its absorption coefficient ($\Phi_T\varepsilon_T$) at a working analysis wavelength, and independent measurements of ε_T. The other way of obtaining the intersystem crossing quantum yield is by means of laser-induced-optoacoustic-spectroscopy (LIOAS) determinations. The use of these techniques is discussed in our previous publication [22]. Briefly, in the LFP experiments the product $\Phi_T\varepsilon_T$, where ε_T is the absorption coefficient of the triplet at the working wavelength, was measured by LFP with ZnTPP (zinc tetraphenyl porphyrin) in benzene as actinometer. The absorption coefficients were determined by the ground state depletion (GSD) method [42]. The second method used to determine the triplet yield of the dyes was LIOAS. The dye Evans Blue was used as a calorimetric reference. An average value of the prompt heat release q was determined from the ratio of the signal amplitude of the reference and the sample. It includes contributions from vibrational relaxation $S_1{}^n \rightarrow S_1{}^o$, nonradiative deactivation $S_1 \rightarrow S_0$, and $S_1 \rightarrow T_1$ transition. In our irradiation conditions only the triplet state of the dyes was formed as an energy storage species and the energy balance may be written as

$$E_\lambda = q + \Phi_F E_S + \Phi_T E_T \quad (14)$$

In Eq. (14) E_λ is the energy of the laser photon at 532 nm, $\Phi_F E_S$ (Φ_F is the fluorescence quantum yield and E_S the first excited singlet energy) is the fraction of energy lost as fluorescence from the singlet state of the dyes, and $\Phi_T E_T$ (E_T is the triplet state energy) is the energy stored by triplet state of the dyes. Using the values of Φ_F, E_S and E_T from the literature, Φ_T could be determined from the experimental q values.

The values of the triplet quantum yield determined by both methods coincide within the experimental error (±20%), and with those in the literature when available [26,43–45]. They are collected in Table 2.

Table 2
Photophysical parameters of xanthene dyes in water, pH 9.5.

Dye	τ_S, ns	${}^1k_q \times 10^{-9}$ $M^{-1}\ s^{-1}$	Φ_T^o	${}^3k_q \times 10^{-7}$ $M^{-1}\ s^{-1}$	Φ_{rad}[c]
Mercury dibromofluorescein	2.01	2.2	0.40	3.6	0.23
Eosin Y	1.19	3.4	0.61	4.2	0.25
Rose Bengal	0.1[a]	–	0.93	6.4	0.15
Erythrosine B	0.1[a]	–	0.97	3.8	0.15
4,5-Dibromofluorescein	2.31	1.4	0.49	3.5	0.22
Fluorescein	4.28	1.4	0.05[b]	–	–
Rhodamine 6G	4.46	0.86	0.1[b]	–	–

[a] Ref. [26].
[b] Ref. [37].
[c] At 20 mM TEOHA.

3.4. Triplet state quenching and radical yield

In the presence of TEOHA a shortening of the triplet lifetime of the dyes was observed. Fig. 4 shows the absorption spectra of

mercury dibromofluorescein at 1 μs and 20 μs after the laser pulse. At 1 μs, it is observed the two absorption bands corresponding to the triplet state. At longer times the absorption in the region 535–600 nm and 330–400 nm is greatly reduced and a new band at 390 nm appears. The inset in Fig. 4 shows that the signal at 560 nm decays with a first order kinetics, and the signal at 400 increases with time at a similar rate. This long-lived signal is ascribed to the absorption of the monoprotonated dye radical formed by proton transfer from the amine cation radical, Eq. (10).

The bimolecular quenching rate constants (^3k_q) were evaluated from the experimentally measured pseudo-first-order decay (k_{obs}) at the longer wavelength absorption band, according to

$$k_{obs} = k_o + {}^3k_q[\text{TEOHA}] \tag{15}$$

where k_o is the triplet decay rate constant in the absence of amine. The values of ^3k_q for the xanthene dyes are included in Table 2. These data show that the triplet quenching by TEOHA is a slow process. Values in the same order of magnitude have been previously reported for eosin and erythrosin in water [46]. However, these values are almost two orders of magnitude lower in organic media [14,46]. Considering that the triplet deactivation is an electron transfer process, the low values of ^3k_q are those expected from the low energy of the triplet state and the low reduction potential of the xanthene dyes [14,19]. Moreover, this quenching mechanism explains the solvent dependence of ^3k_q. However, due to the long lifetime of the triplet dyes more than 92% of triplets are quenched at the amine concentration (20 mM) used in the polymerization studies. The triplet decay of dyes was also measured in the absence of amine in both water and in the presence of 0.4 M acrylamide. In both cases were obtained similar values. These results indicate that the triplet state of dyes is not quenched by the monomer.

Assuming that the active radicals are formed in equal yield than the semireduced form of the dye, the quantum yield of initiating radicals can be estimated from the long-lived absorbance after the triplet decay in the presence of TEOHA, measured in the laser flash photolysis experiments. The triplet yield extrapolated at time = 0 was employed as an internal actinometer. Accordingly, the radical quantum yield was obtained from Eq. (16)

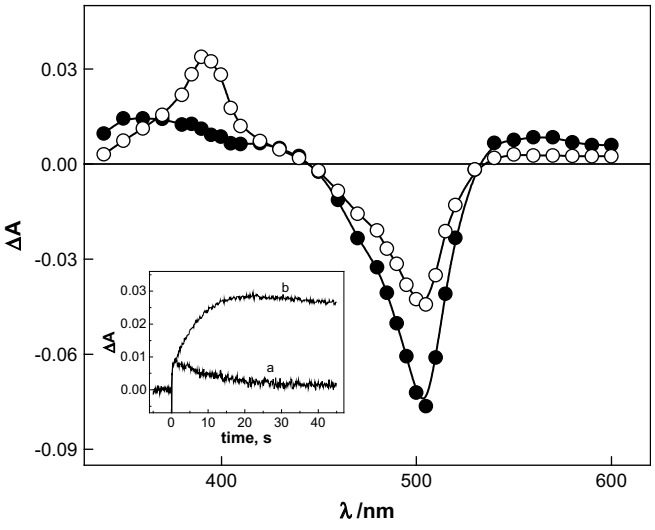

Fig. 4. Transient absorption spectra of mercury dibromofluorescein in the presence of TEOHA 15 mM at (●) 1 μ; and (○) 20 μs. Inset: decay profiles at (a) 560 nm (triplet); (b) 400 nm (radical).

$$\frac{\Delta A_R(t)}{\Delta A_T(0)} = \frac{\Phi_R \varepsilon_R}{\Phi_T \varepsilon_T} \tag{16}$$

where $\Delta A_R(t)$ is the absorbance at the wavelength of the maximum of the transient spectrum of the dye in the presence of TEOHA, measured at time t when all the triplets have disappeared. $\Delta A_T(0)$ is the absorbance at the triplet state extrapolated at time = 0. Φ_T is the triplet quantum yield corrected by the singlet quenching by TEOHA if necessary and ε_R and ε_T are the extinction coefficients of the radical and the triplet, respectively. In order to estimate ε_R the GSD method was employed, $\varepsilon_R = (\Delta A_R/\Delta A_G)\varepsilon_G$ but now the absorption of the radical and ground state is measured when all other transient species have decayed. In this way an estimation of the radical yield could be obtained, albeit its error was difficult to estimate but it must be of considerable magnitude due to the several assumptions made in the procedure. The values are collected in Table 2.

3.5. Photoinitiation mechanism

The polymerization rate is related with the amine radical quantum yield (Eq. (11)), and the fraction of neutral amine radicals that add to the monomer (β) by Eq. (17)

$$\text{Rp}^2 \propto \Phi_{Am^\bullet}\beta \tag{17}$$

Then, the polymerization rate at constant absorbed light and the same monomer concentration can be related to the amine concentration by Eq. (18)

$$\text{Rp}^2 = \text{cte} \quad \alpha \frac{\Phi_T^o}{({}^Sk_q\tau_S^o[\text{Am}] + 1)} \times \frac{{}^3k_q[\text{Am}]}{{}^3k_q[\text{Am}] + k_o} \tag{18}$$

Experimental points shown in Fig. 2 can be represented quite well with Eq. (18) using the measured values of k_q and Φ_T^o. This shows that the radicals that lead to polymerization are those originated from the interaction of the dye triplet with the amine. The singlet deactivation leads to the polymerization inhibition as shown for mercury dibromofluorescein in Fig. 2. At 100 mM TEOHA, 30% of the excited singlets are quenched by the amine. The polymerization is not inhibited using erythrosin as photoinitiator. This is in agreement with the low singlet fraction quenched by the amine (~2%) in concordance with the short singlet lifetime of the erythrosin dye.

Further evidence of the initiation by the radicals formed in the triplet deactivation is the lack of polymerization when fluorescein and rhodamine 6G were employed. The triplet quantum yield for these dyes is lower than 0.1 (Table 2). Although, the 38% of the fluorescein singlets and 28% of rhodamine 6G singlets are deactivated by 100 mM TEOHA, the polymerization was negligible. This is a clear evidence that the active radicals are those formed from the interaction of the triplet excited dye with the amine.

On the other hand, the efficiency as photoinitiator of the different studied dyes can be compared at constant amine concentration; we chose 20 mM TEOHA, because at this concentration all dyes reach the maximum Rp value. As shown in Table 1, Rp values are quite similar for all studied xanthene dyes irrespective on the nature and the number of the substituents at the xanthene ring. Moreover, the xanthene dyes with the larger Φ_T are not better initiators than those with low triplet quantum yields. Relative α values of the fraction of triplet quenched that lead to active radicals (α_{rel}) can be calculated from Eq. (18), taking the measured values of Rp, Φ_T and f_T. These results are shown in Table 3.

Interestingly, data of Table 3 show that the lower α_{rel} values correspond to the dyes with higher Φ_T, Rose Bengal and erythrosin. This means that the main decomposition step of the charge transfer

Table 3
Fraction of the triplet quenched that lead to radicals.

Dye	α_{rel}[a]	α[b]
Mercury dibromofluorescein	1	0.64
4,5-Dibromofluorescein	0.83	0.49
Eosin Y	0.55	0.45
Rose Bengal	0.37	0.16
Erythrosin B	0.37	0.16

[a] Calculated from the measured polymerization rates, Eq. (18).
[b] Calculated from the experimental values of the dye radical quantum yield.

intermediate for these two compounds is the back electron transfer, a process that involves spin inversion. The presence of the heavy atoms, iodine, in the xanthene ring explains the favourable back electron transfer, and then the decrease of the proton transfer in the charge transfer intermediate.

The α values also can be estimated from the experimental values of Φ_T and Φ_{rad} as $\alpha = \Phi_{rad}/\Phi_T$, and are also collected in Table 3. Interestingly, these results, even the high uncertainty in the experimental measurement of the Φ_{rad}, show the same trend than that obtained from the Rp. The trend of α is contrary to that of Φ_T (Table 2). Frequently, it is stated that compounds with high triplet quantum yield are efficient photoinitiators because the active radicals come from the interaction of the triplet state with the co-initiator. However, the factors that increase Φ_T decrease the active radical yield, with the corresponding decrease of the polymerization rate. This explains the similar photoinitiation efficiency that we found for xanthene dyes as photoinitiators of the vinyl polymerization.

4. Conclusions

The detailed study of the processes that deactivate the excited states of xanthene dyes in the polymerization medium allowed to establish a correlation between the efficiency as photoinitiator of xanthene dyes and their photochemical behaviour. Several time-resolved spectroscopies showed that the active radicals are the amine radicals formed in the interaction of the xanthene triplet state with the amine. The measured radical yield is well correlated with polymerization efficiency, however, the photoinitiation efficiency is not correlated with the triplet quantum yield. This shows that to predict the efficiency of the photoinitiator it is necessary to consider all the processes involved in the deactivation of their excited states. Interesting for xanthene dyes, the presence of heavy atoms increases the triplet formation but decrease the radical yield, and then, the polymerization rate.

Acknowledgements

The authors would like to thank FONDECYT-Chile (grant #1070123) and CONICET-Argentina (PIP 5605) and ANPCYT-Argentina (PICTO 30244/05; PICT 32351/05) for financial support of this work.

References

[1] Eaton DF. In: Volman DH, Hammond GS, Gollnick K, editors. Dye sensitized polymerization: advances in photochemistry, vol. XIII. New York: Wiley-Interscience; 1986 [chapter 4].
[2] Monroe BM, Weed GC. Chem Rev 1993;93:435–48.
[3] Jakubiak J, Rabek JF. Polimery 1999;44:447–62.
[4] Fouassier JP, Allonas X, Burget D. Prog Org Coatings 2003;47:6–36.
[5] Neckers DC, Raghuveer KS, Valdes-Aguilera O. Polym Mater Sci Eng 1989;60:15–6.
[6] Fouassier JP, Chesneau E. Makromol Chem 1991;192:245–60.
[7] Sudesh Kumar G, Neckers DC. Macromolecules 1991;24:4322–7.
[8] Mallavia R, Amat-Guerri F, Fimia A, Sastre R. Macromolecules 1994;27:2643–6.
[9] Pączkowski J, Kucybala Z. Macromolecules 1995;28:269–73.
[10] Burget D, Fouassier JP, Amat-Gerri F, Mallavia R, Sastre R. Acta Polym 1999;50:337–46.
[11] Kabatc J, Kucybala Z, Pietrzak M, Ścigalski F, Pączkowski J. Polymer 1999;40:735–45.
[12] Popielarz R, Vogt OJ. Polym Sci Part A Polym Chem 2008;46:3519–32.
[13] Kim D, Scranton AB, Stansbury JW. J Polym Sci Part A Polym Chem 2009;47:1429–39.
[14] Grotzinger C, Burget D, Jacques P, Fouassier JP. Macromol Chem Phys 2001;202:3513–22.
[15] Grotzinger C, Burget D, Jacques P, Fouassier JP. Polymer 2003;44:3671–7.
[16] Hassoon S, Neckers DC. J Phys Chem 1995;99:9416–24.
[17] Polykarpov AY, Hassoon S, Neckers DC. Macromolecules 1996;29:8274–6.
[18] Wrzyszczyñski A, Pietrzak M, Pączkowski J. Macromolecules 2004;37:41–4.
[19] Ścigalski F, Pączkowski JJ. Appl Polym Sci 2005;97:358–65.
[20] Avens HJ, Randle TJ, Bowman CN. Polymer 2008;49:4762–8.
[21] Borsarelli CD, Bertolotti SG, Previtali CM. Photochem Photobiol Sci 2002;1:574–80.
[22] Broglia MF, Gómez ML, Bertolotti SG, Montejano HA, Previtali CM. J Photochem Photobiol A Chem 2005;173:115–20.
[23] Previtali CM, Bertolotti SG, Neumann MG, Pastre IA, Rufs AM, Encinas MV. Macromolecules 1994;27:7454–8.
[24] Encinas MV, Rufs AM, Neumann MG, Previtali CM. Polymer 1996;37:1395–8.
[25] Villegas L, Encinas MV, Rufs AM, Bueno C, Bertolotti SG, Previtali CM. J Polym Sci Part A Polym Chem 2001;39:4074–82.
[26] Fleming GR, Knight AWE, Morris JM, Morrison RJS, Robinson GW. J Am Chem Soc 1977;99:4306–11.
[27] Korobov VE, Chibisov AK. Russ Chem Rev 1993;52:27–42.
[28] Zhao ZG, Xu HJ, Shen T. J Photochem Photobiol A Chem 1991;56:73–80.
[29] del Valle JC, Catalán J, Amat-Guerri F. J Photochem Photobiol A 1993;72:49–53.
[30] Zakrzewski A, Neckers DC. Tetrahedron 1987;43:4507–12.
[31] Neckers DC, Hassoon S, Klimtchuk E. J Photochem Photobiol A Chem 1996;95:33–9.
[32] Orellana B, Rufs AM, Encinas MV, Previtali CM, Bertolotti SG. Macromolecules 1999;32:6570–3.
[33] Valdebenito A, Encinas MV. J Polym Sci A Polym Chem 2003;41:2368–73.
[34] Klimtchuk E, Rodgers MAJ, Neckers DC. J Phys Chem 1992;96:9817–20.
[35] Jain K, Klier J, Scranton AB. Polymer 2005;46:11273–8.
[36] Valdebenito A, Encinas MV. J Photochem Photobiol A Chem 2008;194:206–11.
[37] Magde D, Wong R, Seybold PG. Photochem Photobiol 2002;75:327–34.
[38] Cramer LE, Spears KG. J Am Chem Soc 1978;100:221–7.
[39] Magde D, Rojas GE, Seybold P. J Photochem Photobiol 1999;70:737–44.
[40] Burget D, Fouassier JP. J Chem Soc Faraday Trans 1998;94:1849–54.
[41] Islam SDM, Konishi T, Fujitsuka M, Ito O, Nakamura Y, Usui Y. J Photochem Photobiol 2000;71:675–80.
[42] Carmichael I, Hug GL. J Phys Chem Ref Data 1986;15:1.
[43] Bowers PG, Porter G. Proc R Soc A 1967;299:348–53.
[44] Mau AWH, Johansen O, Sasse WHF. Photochem Photobiol 1985;41:503–9.
[45] Görner H. Photochem Photobiol Sci 2008;7:371–6.
[46] Islam SDM, Yoshikawa Y, Fujisuka M, Watanabe A, Ito O. Bull Chem Soc Jpn 1998;71:1543–8.